Variable Step-Size Decremented Window-Size Scanning-based MPPT Algorithms for Thermoelectric Generator Systems

Conference Paper · April 2018

DOI: 10.1109/AEMT.2018.8572407

CITATIONS
3

READS
21

3 authors:

Faizal Arya Samman
Universitas Hasanuddin
72 PUBLICATIONS **375** CITATIONS
SEE PROFILE

Wahyu H. Piarah
Universitas Hasanuddin
49 PUBLICATIONS **222** CITATIONS
SEE PROFILE

Zuryati Djafar
Universitas Hasanuddin
47 PUBLICATIONS **130** CITATIONS
SEE PROFILE

Variable Step-Size Decremented Window-Size Scanning-based MPPT Algorithms for Thermoelectric Generator Systems

Faizal Arya Samman[1]
Universitas Hasanuddin, Faculty of Engineering
[1]Dept. of Electrical Engineering
Jl. Poros Malino Km. 6, Bontomarannu, Gowa 92171
Email: faizalas@unhas.ac.id[1]

Wahyu H. Piarah[2], Zuryati Djafar[3]
Universitas Hasanuddin, Faculty of Engineering
[2,3]Dept. of Mechanical Engineering
Jl. Poros Malino Km. 6, Bontomarannu, Gowa 92171
Email: wahyupiarah@unhas.ac.id[2], zuryatidjafar@unhas.ac.id[3]

***Abstract*—Variable Step-Size Decremented Window-Size Scanning-based MPPT Algorithms for Thermoelectric Generator Systems are presented in this paper. The proposed MPPT algorithm is simple to implement and can tune automatically the TEG system to operate at its maximum power point effectively. By using different step-size decrements and step-number changes for each scanning-step iteration, four types of DWS-based MPPT algorithms are derived. The performance of the four DWS algorithms are verified through simulations. The optimal or appropriate selection of the variable step-size decrements for each scanning-step iteration can improve the convergence speed of the algorithms to reach the expected maximum power points. The DWS-based MPPT algorithm, which uses for example a 13-4-1 step-size decrement with 1% minimum duty-ratio step-size, can reach the maximum power point after 22 P&O-steps. The need for relatively small number of the required P&O-steps, in addition to the simple computing implementation, is the impressive features of the proposed DWS-based MPPT algorithms for thermoelectric-based energy harvesting applications.**

Keywords*—Power Electronics, Digital Control, Maximum Power Point Tracking Algorithm, Thermoelectric Generator, Renewable Energy, Thermal Energy Harvesting.

I. Introduction

In recent decade, renewable energy has been a prominent issue due to the decrease of fossil fuel resources in the earth and the environment aspect. There are many renewable energies that can be potentially used as energy resources for electric power plants in the future such as solar, wind, tidal, geothermal. Hydro, including micro-hydro power plants that use also renewable energy, have been utilized in current power systems. The progressive improvement of the efficiency of solar or photovoltaic (PV) cells will potentially accelerate the utilization of PV-based electric power generation.

Meanwhile, exhausted heats are found every where in our daily life and industries. These exhausted thermal energies can be found, for instances, from combustion engine bodies in automotive and industries, from the metal-made or alloy-made rooftops of houses, from exhaust gas pipes in automotive, and from many other exhausting heat sources due to the sun radiation, thermal conductions from combustion processes, or even due to super large scale computation in a supercomputer station. These exhausted energy are also potential energy sources. By using, for example, thermoelectric generator (TEG) devices, the exhausted energies electric energy can be recovered to be electric energy.

This paper will discuss about the thermal energy harvesting using TEG patches or panels. On the left-hand side of Fig. 1, a thermo mechanical model of a TEG is presented. The temperature difference between two sides of the TEG patch, due to heat flows, will trigger the semiconductor materials between the both sides to generate electric power. A TEG patch has specific power characteristic, where it maximum power transfer is located on a certain current point. Therefore, it is necessary to operate the TEG patch at that point. This paper proposes a technique to maximize the power delivery of the TEG by using effective and low complex maximum power point tracing (MPPT) algorithms.

To achieve the objectives and to expose the main idea of this research paper clearly, the paper are organized in the following sections. Section II presents the research works related to the MPPT techniques for TEGs. To understand well the power characteristics of the TEGs, the thermal mechanical and its equivalent electric circuit models are explored, as presented in Section III. By using SPICE simulator, the models are simulated to obtain the TEG's power curves. From the power curve figures, the maximum power point can be observed. Section IV exposes the proposed MPPT algorithms, namely decremented window-size scanning-based MPPT algorithm. The power curves data from the previous section are reconstructed using a numerical computing software tool. The MPPT algorithms are then tested and simulated using the software tool to analyse their performance as presented in Section V. The concluding remarks and outlooks are finally presented in Section VI.

II. Related Works and Contribution

MPPT algorithm for Thermoelectric Generator (TEG) systems can be implemented using digital or analog electronic control unit (ECU) [1]. The analog MPPT control unit is simple and has low cost design, but it has a few drawbacks. One of them is its sensitivity to the drifts of component parameters and external noise signals. Our proposed MPPT algorithms can be implemented in digital programmable electronic control unit such as microcontroller and programmable logic device families. As we know, the digital techniques are more robust

to the parameter drifts and noises compared to the analog techniques.

There are some techniques that can be used to maintain TEG operates at its maximum power point, such as P&O methods, fractional open-circuit voltage [2], and fractional short-circuit current [3]. The fractional open-circuit voltage (OCV) and fractional short-circuit current (SCC) is simple, but for different TEG operating conditions and TEG structures, the open-circuit voltage or the short-circuit current, which are needed to know in advanced before implementation, must be measured again. Hence, the flexibility of the fractional OCV and fractional SCC are very low. The work in [4] uses only charge pump and voltage regulator devices, without an MPPT algorithm, to control the TEG's output voltage. Hence, the approach is only suitable for low energy harvesting application with fixed TEG configuration.

We propose P&O-based techniques that are independent from the operating condition and TEG structure changes, resulting in a highly flexible MPPT algorithm design. The proposed algorithms is called as Decremented Window-Size Scanning (DWS) based MPPT algorithms. The previous version of the proposed MPPT algorithm has been successfully tested in a photovoltaic system model [5]. These current proposed algorithms can also successfully be applied to TEG system models as presented in this paper, with additional contribution to the improvement of the convergence speed. A new approach by varying the duty-ratio step-number and step-size decrements is proposed and used to improve the trace speed of the algorithms to reach the expected maximum power points.

III. TEG Modelling and Power Characteristics

Before, the proposed DWS-based algorithms are applied to the TEG system through simulations, there are some stages that should be followed, i.e. the modelling of a single TEG patch and an array of TEG patches in an equivalent electric circuit diagram. This model is useful to achieve the TEG's power characteristics, and the most important thing is that the model can be simulated with a DC/DC converter circuit (used to implement the MPPT algorithm) in SPICE simulation environment. Moreover, for further research objective, the TEG model can also be used to optimize the design structure of TEG device [6].

SPICE (Simulation Program with Integrated Circuit Emphasis) is an industry-standard software used to model and simulate electric and electronic circuits. The TEG is modelled in SPICE program, and then is simulated to obtain its power curve profile. The following subsections describe the simulation results.

A. Single TEG Patch Model

The TEG patch can be modelled in an equivalent electric circuit as presented in Fig. 1. The figure on the left-hand side presents the thermo mechanical diagram. While, the one on the right-hand side shows the equivalent electric circuit diagram. The TEG patch is modelled in a single wire loop with a variable voltage source (V_{EQ}) in series with a variable resistor (R_{EQ}). Both variables are the function of the temperature difference between the hot and cold side of the TEG (ΔT). The

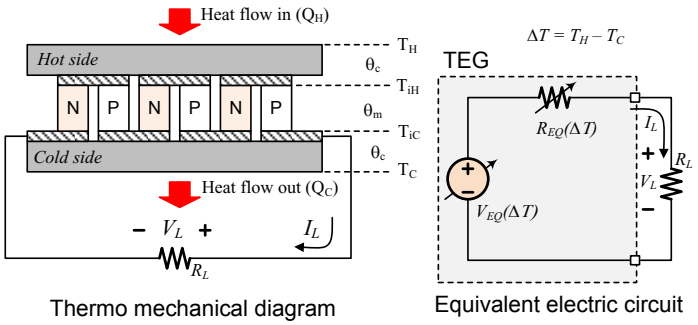

Fig. 1. Single TEG patch and its equivalent electric circuit model.

variable voltage source and the variable resistor are formulated as in Eq. (1) and Eq. (2), respectively [7].

$$V_{EQ} = \alpha \Delta T \frac{\theta_m}{\theta_m + 2\theta_c} \tag{1}$$

$$R_{EQ} = R_E + \alpha^2 \theta_m \theta_c \frac{T_H + T_C}{\theta_m + 2\theta_c} \tag{2}$$

The parameters of the equations are described as follows:

- α : Seebeck coefficient, depends on the P-N semiconductor material
- θ_m : internal thermal resistance
- θ_c : contact thermal resistance, which is the contact is used to connect the TEG panel to the thermal energy source
- R_E : electric resistance, consists of P-N semiconductor resistance and contact resistance, which is the contact used to connect the TEG panel and the load

The temperature difference between the hot and cold side of the TEG is written as follows.

$$\Delta T = T_H - T_C \tag{3}$$

By substituting Eq. (3) into Eq. (2), then we will have Eq. (4) as follows.

$$R_{EQ} = R_E + \alpha^2 \theta_m \theta_c \frac{\Delta T + 2T_C}{\theta_m + 2\theta_c} \tag{4}$$

By modelling and simulating Eq. (1) and Eq. (4) in SPICE and using the TEG parameters shown in Table I, the power curve profile of the TEG is obtained as shown in Fig. 2. It seems that larger temperature difference will result in larger output power. Each power curve presents also a peak or maximum power point. The power curve profiles illustrate that for each temperature condition there is a current point (or voltage point in other case), in which the TEG will deliver a maximum power. This point is called a maximum power point that should be targeted operation point of the TEG. This is the basic idea of introducing a maximum power point tracing (MPPT) algorithm that is used to drive the TEG to operate at the expected maximum power point. This issue is discussed later in Section IV.

TABLE I. THE TEG PARAMETERS VALUE USED IN THE SIMULATIONS.

Parameter	Value
α	0.0531876
θ_m	1.498 K/W
θ_c	0.45 K/W
R_E	1.6 Ω

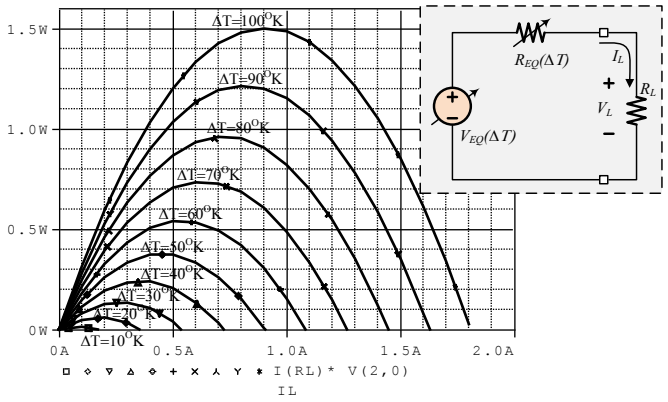

Fig. 2. Single TEG equivalent circuit model and its power curve characteristic.

B. TEG Patch Array Model

In this section, the power curve characteristic of a TEG patch arrangement in array structure of 2×4, i.e. two parallel branches, where each branch consists of four TEG patch connected in series, is presented. Fig. 3 presents the power curve characteristic. Larger temperature differences (ΔT) results in higher maximum powers. Similar to the previous simulation result, larger temperature difference results in larger output power, and every power curve has a peak or maximum output power at certain electric current point.

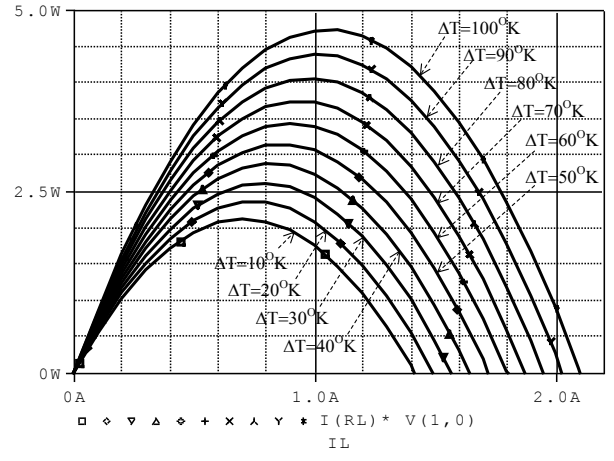

Fig. 3. TEG patch array (2×4) power curve characteristic.

C. TEG Patch Array Power Profile with SEPIC Circuit

After having the power curve profiles of the TEG in an array structure, we will discuss here techniques to maintain the TEG operation at its maximum power point. In order to control the TEG current or voltage, a switched-mode DC/DC converter is required. This DC/DC converter is actually used to change the output impedance of the TEG in such a way that the impedance will match with load impedance. The matching process is made by applying a pulse width modulated (PWM) signal to the gate terminal of MOSFET in the DC/DC converter. When the matching takes place, then the maximum power transfer to the load is accomplished.

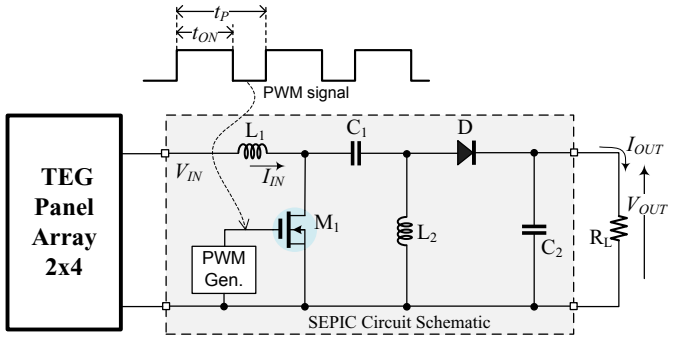

Fig. 4. The SEPIC circuit connected to the output terminal of the TEG array.

There are some types of DC/DC converters that can be used in this case. One of them is a single-ended primary inductive converter or generally named as SEPIC [8] [9]. The circuit topology of the SEPIC is presented in Fig. 4. The SEPIC input terminal is connected to the TEG and its output terminal is connected to the load R_L. As presented in the figure, the PWM signal, having period of t_P with t_{ON} duty cycle, is applied to the MOSFET M_1 gate terminal. The duty ratio of the PWM signal is $\frac{t_{ON}}{t_P} \times 100\%$.

When the load R_L is set 50Ω and 100Ω, and the ΔT is set 100^oK, the SEPIC, the load and the TEG are simulated by changing the duty ratio of the PWM signal from 10% until 90%. Fig. 5 presents the power curve characteristic of the SEPIC and TEG output terminals as the simulation result. As shown in the figure, it seems that there is a duty ratio point, where the TEG and SEPIC output power will be maximally transferred to the load R_L. We can also see that the maximum (duty-ratio/power) point is different for different load values.

As shown in Fig. 5, the maximum power point for the case of $R_L = 50\Omega$ is about 8.05W at 76% PWM duty ratio, and for the case of $R_L = 100\Omega$ is about 8.05W at 80% PWM duty ratio. But, the main big question is, who will drive the duty ratio of the PWM signal such that it will automatically end up at the expected duty ratio? The answer is that we need a control algorithm which is embedded on an electronic control unit. Fig. 6 illustrates the SEPIC circuit accompanied with an electronic control unit (ECU).

IV. THE DWS-BASED MPPT ALGORITHMS

As shown in Fig. 6, the MPPT algorithm is embedded (implemented) on the ECU. The output (load) voltage (V_{OUT}) and current (I_{OUT}) are measured using voltage/current sensors. Multiplying both DC signals, we get the power signal (P_{OUT}). The ECU, in which the MPPT algorithm is embedded, will perturb the SEPIC with a PWM signal having a certain duty ratio. Then, the ECU observes the SEPIC output power from the voltage-current measurement and multiplication. For each perturb repetition, the ECU will observe the power and

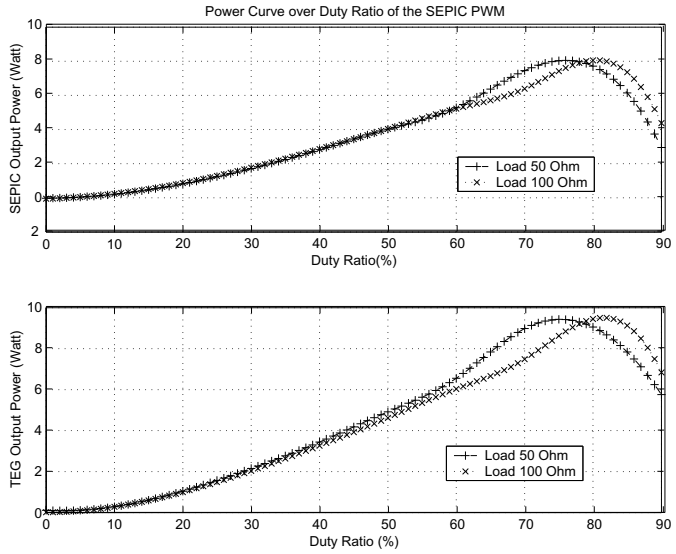

Fig. 5. The TEG patch array power curve characteristic with different duty ratio.

compare it with the previous one, and record the tentative maximum power and duty ratio point for every P&O step. By iteratively doing so, the maximum power point will be finally found. The detail descriptions of the proposed MPPT algorithms, which we called as Decremented Windows-Size Scanning-based (DWS), is discussed in this section.

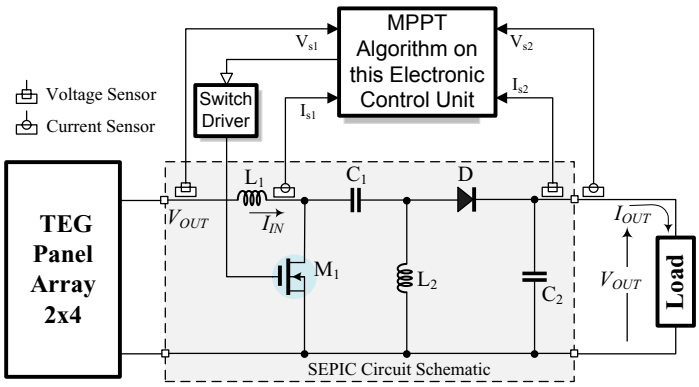

Fig. 6. The simulation setup of the MPPT module with SEPIC and TEG patch array.

The DWS-based MPPT algorithm is simple to implement and can derived into several modes. The window or the domain of P&O scanning of the algorithm is reduced for each iteration scan. Accordingly, the step-size and the step number of the P&O scanning process variably change in every scan step. Based on the decremented step size, this algorithm is called decremented window-size scanning.

We proposed four approaches (methods) to implement the DWS algorithms, where each of them has different step-size decrement and step number for each scanning iteration. The differences of the DWS algorithm are summarized in Table II. The step-size decrement is order of the step-size that is decremented for the next or each P&O scan-step iteration. By using the DWS method 2 for example, the step-size decrement values are 10-4-2-1 (4 ordered decrement values). It means that for every P&O scan-step iteration, the step-size values are variably decremented from 10, 4, 2 and 1 duty ratio step-size. The minimum density of the step-size is 1% duty ratio. The step number is the number of P&O step undertaken for each scan-step iteration. The number of scan-step iteration is related to the the number of ordered step-size decrement values.

TABLE II. THE DIFFERENCE OF THE PROPOSED DWS-BASED MPPT ALGORITHMS.

Method	Step-Size Decrement	Step-Number Change	Number of Scan-Step Iterations
DWS method 1	20-10-5-2-1	5-5-5-5-5	5
DWS method 2	10-4-2-1	9-6-5-5	4
DWS method 3	10-1	9-19	2
DWS method 4	13-4-1	7-7-7	3

V. SIMULATION RESULTS

In this section, the proposed DWS algorithms are tested through simulations to track the maximum power points of the power curves presented previously in Fig. 5, i.e. the power curves for the TEG system with load resistance of 50Ω and 100Ω.

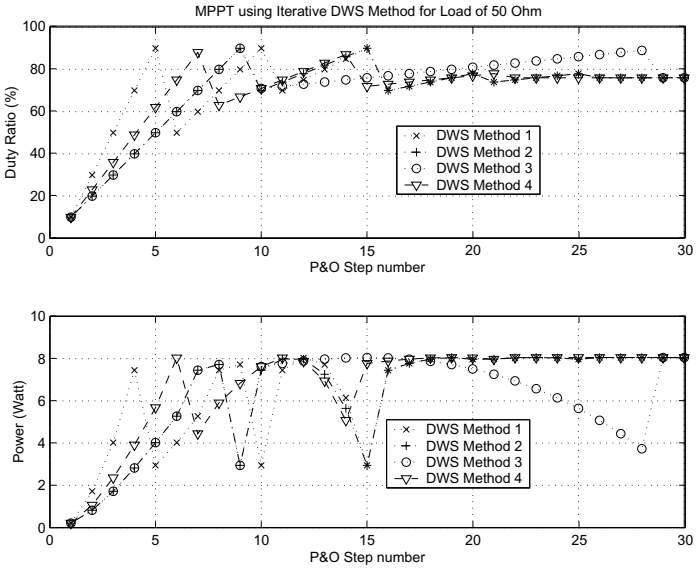

Fig. 7. The simulation results for 50 Ohm resistance load.

Fig. 7 presents the simulation result for 50Ω resistance load value. As shown in the figure, the four DWS algorithms can attain the same maximum power point, i.e. about 8.0524 Watt at 76% PWM's duty ratio point, although they have different power and duty ratio tracking lines. The performances of the DWS-based MMPT algorithms are summarized later in Table III.

Fig. 8 shows the simulation result for 100Ω resistance load value. As presented in the figure, the four DWS algorithms can again attain the same maximum power point, i.e. about 8.0538 Watt at 80% PWM's duty ratio, with different power and duty ratio tracking lines. It seems also that the DWS method 1, 2 and 4 can trace the maximum power point faster than the DWS method 3.

From both simulation results, we have seen how all of the DWS algorithms can tune automatically the duty ratio of

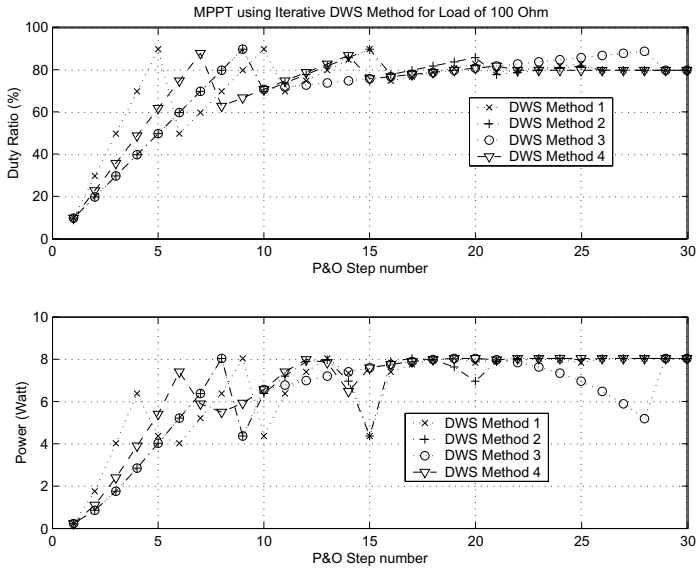

Fig. 8. The simulation results for 50 Ohm resistance load.

the PWM signal at an expected point such that the power output of the TEG system can be traced accordingly to the expected maximum point. Table III presents the performance comparison between the DWS-based MPPT algorithms for load resistance value of 50Ω. The table shows the reached output power at final duty ratio of the PWM signal, i.e. the maximum power point (MPP), as well as the number of P&O-steps to reach the MPP. The DWS method 4 outperforms the other DWS methods in term of the convergence speed. The DWS method 4 requires the least number of P&O-steps, i.e. 22 step, to reach the MPP. The worst performance is presented by the DWS method 3. It requires 29 P&O-steps to reach the MPP. All methods however can reach the same output power, i.e. 8.0524W at the PWM duty ratio of 76%.

TABLE III. THE PERFORMANCE COMPARISON OF THE DWS-BASED MPPT ALGORITHMS.

Method	Reached Power	Final Duty Ratio	Number of P&O-steps
DWS method 1	8.0524W	76%	26
DWS method 2	8.0524W	76%	26
DWS method 3	8.0524W	76%	29
DWS method 4	8.0524W	76%	22

For the case of the resistance load of 100Ω, the same performance is obtained. The DWS method 1, 2, 3 and 4 require different number of P&O-steps to reach the MPP. Each of them requires respectively 26, 26, 29 and 22 steps. However, all DWS methods can reach the same maximum power point, i.e. 8.0538W, and the same duty ratio point, i.e. at 80%.

VI. CONCLUSIONS

This paper has presented four DWS-based MPPT algorithms, which operate based on iterative variable step-size and step-number scanning-based P&O technique. Since the window or the domain of scanning is reduced for each iteration scan, then the step-size and the step number of the scanning process variably change in every scan step. The optimal selection of the variable step-size decrements for each P&O scanning step can improve the convergence speed of the algorithms to reach the expected maximum power point (MPP).

By using the proposed methods, the expected maximum power point will be finally trapped in this gradually reduced domain scan with relatively small number of P&O-steps. The proposed DWS-based MPPT methods can reach the maximum power point at about 22 until 28 P&O-steps in case of using 1% minimum duty-ratio step-size. The minimum duty ratio step-size can be further reduced to a lower number. The selected lower values could probably only result in slightly small MPP accuracy improvements. But, it will reduce the convergence step due to a more complex algorithm.

In addition to the aforementioned advantageous features, the DWS-based MPPT algorithm are simple and flexible to implement. The implementation is more flexible compared to fractional OCV and fractional SCC, because it does not require prior information about the TEG's configuration and load conditions. Under different load conditions, the proposed techniques can tune automatically the duty-ratio of the PWM signals exactly at the expected maximum power point.

ACKNOWLEDGMENT

We gratefully acknowledge Universitas Hasanuddin at Makassar for funding this research work under the scheme of the Excellent Research Grant for Patent Publication (*Penelitian Unggulan Berpotensi Paten*) in the year 2017.

REFERENCES

[1] S. Kim, S. Cho, N. Kim, and J. Park, "A maximum power point tracking circuit of thermoelectric generators without digital controller," *IEICE Electronics Express*, vol. 7, no. 20, pp. 1539–1545, Oct. 2010.

[2] A. Montecucco and A. R. Knox, "Maximum Power Point Tracking Converter Based on the Open-Circuit Voltage Method for Thermoelectric Generators," *IEEE Trans. on Power Electronics*, vol. 30, no. 2, pp. 828–839, Feb. 2015.

[3] I. Laird and D. D. Lu, "High Step-up DC/DC Topology and MPPT Algorithm for use with a Thermoelectric Generator," *IEEE Trans. on Power Electronics*, vol. 28, no. 7, pp. 3147–3157, July 2013.

[4] W. Wang, V. Cionca, N. Wang, M. Hayes, B. O'Flynn, and C. O'Mathuna, "Thermoelectric Energy Harvesting for Building Energy Management Wireless Sensor Networks," *International Journal of Distributed Sensor Networks*, vol. 2013, pp. 1–14, Article ID 232 438, 2013.

[5] F. A. Samman, A. A. Rahmansyah, and Syafaruddin, "Iterative Decremented Step-Size Scanning-based MPPT Algorithms for Photovoltaic Systems," in *Proc. of the 9th Int'l Conf. on Information Technology and Electrical Engineering (ICITEE 2017)*, 2017.

[6] H. Chen, N. Wang, and H. He, "Equivalent Circuit Analysis of Photovoltaic-Thermoelectric Hybrid Device with Different TE Module Structure," *Advances in Condensed Matter Physics*, vol. 2014, pp. 1–6, Article ID 824 038, 2014.

[7] S. Siouane, S. Jovanovi, and P. Poure, "Equivalent Electrical Circuits of Thermoelectric Generators under Different Operating Conditions," *Energies, MDPI Journal*, vol. 10, pp. 1–15, July 2017.

[8] E. Babaei and S. M. E. Mahmoodieh, "Calculation of Output Voltage Ripple and Design Consideration of SEPIC Converter," *IEEE Trans. on Industrial Electronics*, vol. 61, no. 3, pp. 1213–1222, March 2013.

[9] G. Tian and et al., "High Power Factor LED Power Supply based on SEPIC Converter," *IET Electronics Letters*, vol. 50, no. 24, pp. 1866–1868, 2014.